Published in final edited form as:
Microcirculation. 2012 May ; 19(4): 360–372. doi:10.1111/j.1549-8719.2012.00172.x.

Characterization of the thoracodorsal artery: morphology and reactivity

Marie Billaud[1], **Alexander W Lohman**[1,2], **Adam C Straub**[1], **Thibaud Parpaite**[1], **Scott R Johnstone**[1], and **Brant E Isakson**[1,2,*]

[1]Robert M. Berne Cardiovascular Research Center, University of Virginia School of Medicine, P.O. Box 801394, Charlottesville, VA 22908

[2]Department of Molecular Physiology and Biological Physics, University of Virginia School of Medicine

Abstract

In this paper, we describe the histological and contractile properties of the thoracodorsal artery (TDA), which indirectly feeds the spinotrapezius muscle. Our results demonstrate that the TDA is composed of approximately one-two layers of smooth muscle cells, is highly innervated with adrenergic nerves, and develops spontaneous tone at intraluminal pressures above 80 mmHg. The reactivity of the TDA in response to various contractile agonists such as phenylephrine, noradrenaline, angiotensin II, serotonin, endothelin 1 and ATP as well as vasodilators show that the TDA exhibits a remarkably comparable reactivity to what has been observed in mesenteric arteries. We further studied the different components of the TDA response to acetylcholine and found that the TDA was sensitive to TRAM 34, a blocker of the intermediate conductance potassium channel, which is highly suggestive of an endothelium-dependent hyperpolarization. We conclude that the TDA exhibits comparable characteristics to other current vascular models, with the additional advantage of being easily manipulated for molecular and *ex vivo* vasoreactivity studies.

Keywords

Vascular model; Vasoreactivity

Introduction

The role of the skeletal muscle arteriolar network in the regulation of muscle blood flow is particularly important during skeletal muscle contraction. In addition to the arteriolar microvessels within the skeletal muscle, the terminal feed arteries, which are not encased in the skeletal muscle, participate in the increased blood flow following muscle contractions (45, 46, 66). The skeletal muscle arteriolar network has been studied using intravital microscopy performed on several mouse preparations, including the gluteus maximus muscle, the cremaster muscle and the spinotrapezius muscle (1–4, 34, 44, 52, 65, 73).

The use of spinotrapezius muscle preparations were first described by Gray in 1973 and since then, the arteriolar network of the rat spinotrapezius muscle, as well as the proximal arteries feeding this muscle, has been extensively described and functionally characterized by Schmid-Schönbein and Zweifach in a series of publications (24, 61, 64, 65). In this regard, important insights in the function of the spinotrapezius muscle microcirculation have

*To whom correspondence should be addressed: Phone: 434-924-2093, Fax: 434-924-2828, brant@virginia.edu.

been achieved in health and diseases (9, 44). However, the isolation of the arterioles within the spinotrapezius muscle microcirculation has proven to be difficult due to their anatomical location. We therefore hypothesized that examination of the upstream arteries, which are more directly accessible to isolation, may provide an adequate vascular model system.

Similarly to its equivalent in the hamster (the retractor muscle), the mouse spinotrapezius muscle is supplied by main feed arteries directly originating from an artery termed the thoracordorsal artery (TDA) (16). Anatomically, the TDA is a branch of the subscapular artery which arises from the axillary artery, a continuation of the subclavian artery originating at the aortic arch. The TDA accompanies the thoracodorsal nerve to the lateral border of the scapula which respectively supply and innervate that muscle region (41) including the spinotrapezius muscle (64), the latissimus dorsi and the serratus anterior muscles (15), the interscapular brown adipose tissue and the skin (21). Although the TDA studied in the present paper is not a terminal feed artery of the spinotrapezius muscle, its contribution to functional hyperemia in the rat spinotrapezius muscle has been suggested (44). Indeed, Lash demonstrated that the upstream resistance of the spinotrapezius muscle, consisting of the resistance of the arteries supplying flow to the feed arteries, including the TDA, is significantly decreased during contraction of the spinotrapezius muscle (44). More recently, evidence has indicated that the blood flow measured in the TDA is increased during systemic hypoxia in rats, along with a decrease of TDA vascular resistance with a drop of mean arterial pressure (31). These findings suggest the physiological implication of the TDA in vascular functions and indicate that this artery may be particularly useful as a vascular model system.

The purpose of this study was to carry out *ex vivo* studies of the mechanical and physiological properties in the TDA including its histological description, the incidence of myogenic tone and the reactivity to common vasoactive agents. In addition, the components of the endothelium dependent relaxation to acetylcholine were studied. Our data imply that, although anatomically the TDA is not a resistance artery, morphologically (e.g., the presence of MEJs, 1 to 2 layers of smooth muscle cells), functionally (the presence of an L-NAME/indomethacin insensitive relaxation to Ach and identical reactivity to second order mesenteric arteries) and its role in feeding a load-bearing skeletal muscle show that this artery is a valid vascular model system.

Material and methods

Animal

Male mice (12–16 weeks), strain C57Bl/6 were purchased from Taconic (Germantown, NY) and used according to the University of Virginia Animal Care and Use Committee guidelines.

Dissection of the thoracodorsal artery

Mice were sacrificed using CO_2 asphyxia, placed in the lateral decubitus position and the scapular area was sprayed with ethanol 70%. A 3 to 4 cm incision was performed and the skin was carefully removed without affecting the superficial dorsal muscle underneath. Tissues were constantly humidified with cold Krebs-HEPES containing (in mM) NaCl 118.4, KCl 4.7, $MgSO_4$ 1.2, $NaHCO_3$ 4, KH_2PO_4 1.2, $CaCl_2$ 2, Hepes 10, glucose 6 and supplemented with 1% BSA. The removal of the skin revealed the superficial layers of the dorsal musculature including the spinotrapezius muscle, the latissimus dorsi muscle and triceps brachii muscle (forelimb, Figure 1A, B). Using microdissection while viewing through a stereomicroscope (SZ61, Olympus), the latissimus dorsi muscle was removed to access to the TDA underneath, lining the caudal side of the scapula (Figure 1C, D). The

TDA is surrounded by fat tissue and by two veins (Figure 1E) which were carefully dissected. Once free of surrounding tissues, about 10 to 15 mm length of the TDA was isolated, cut in 3 smaller pieces for cannulation experiments and placed in cold Krebs-HEPES to be used for up to 8 hours.

Histology

Mice were sacrificed using CO_2 asphyxia, placed in the dorsal decubitus position. The chest was opened and a 25G needle mounted on a syringe containing Krebs-HEPES calcium free + heparin (10 units/ml) was placed in the left ventricle of the heart and the right ventricle was incised simultaneously. After perfusing 5 ml of the solution, the syringe was replaced by a syringe containing 4% paraformaldehyde (PFA). After the PFA was perfused, the TDA was isolated as described above, placed in 4% PFA for 1 hour at 4°C and then placed in 70% ethanol until paraffin embedding. Paraffin blocks were processed for sectioning of 4–5μm thick transverse sections, which were further stained with hematoxylin and eosin where indicated.

Immuofluorescence

Mice were perfused transcardially as described above, TDA were isolated, placed for 30 minutes in blocking solution and incubated overnight with primary antibody (anti-tyrosine hydroxylase 1/1000, Abcam; anti-nNOS 1/200, Abcam) at 4°C. The TDA was washed in PBS and incubated with the corresponding secondary antibody coupled to Alexa Fluor 488 or Alexa Fluor 594 for 2 hours at room temperature. The TDA was washed in PBS, mounted in DAPI ProLong Gold Antifade reagent (Invitrogen) and imaged with an Olympus Fluoview 1000 confocal microscope.

Transmission Electron Microscopy

Mice were perfused transcardially as described above with 4% PFA + 2.5% glutaraldehyde. The TDA was isolated, fixed with 1% osmium tetraoxide followed by dehydration in a gradient of alcohol and embedding in Epon. Ultrathin sections (75 nm) were cut, carbon coated and imaged with a JEOL 1230 as previously described (37).

Immunolabelling coupled to scanning electron microscopy

Mice were perfused transcardially as described above with 4% PFA + 0.5% glutaraldehyde, TDA was isolated and the adventitia was removed using 1mg/ml collagenase type VIII (Sigma) and 30% KOH as previously described (6). Vessels were then placed in blocking solution for 30 minutes at room temperature and in primary antibody (anti-NG2, Chemicon) overnight at 4°C. Vessels were washed in PBS and incubated with the secondary antibody coupled to 25nm gold beads. Finally, vessels were fixed with 1% osmium tetraoxide, dehydrated in a gradient of alcohol, coated with gold and visualized with a JEOL 6400 scanning electron microscopy as previously described (6).

Measurements of myogenic tone

The TDA were freshly isolated as described above and mounted in a pressure arteriograph (Danish MyoTechnology) where they were maintained in a no flow state as previously described (6, 67). After 30 minutes of equilibration at 80 mmHg, the TDA were subjected to a gradient of pressure from 10 to 140 mmHg with a 5 minute stabilization period for each pressure to measure the active diameter. The TDA was then incubated in Krebs-HEPES calcium free supplemented with 2mM Ethyleneglycol-O, O′-bis(2-aminoethyl)-N, N, N′, N′-tetraacetic acid (EGTA, Sigma) and 10 μM sodium nitroprusside (Sigma), the intraluminal pressure was set at 80 mmHg for 30 minutes and the gradient of pressure was repeated to measure the passive diameter. The myogenic tone was calculated at each pressure step

following the equation: percent myogenic tone = [(passive diameter − active diameter)/ passive diameter] × 100.

Measurements of contractile properties

The TDA were mounted in a pressure arteriograph as described above and pressurized at 80 mmHg. Vessels were equilibrated for 30 minutes after cannulation and further stimulated with cumulative concentrations of different vasoconstrictor agents: phenylephrine (PE, 10^{-8} to 10^{-4} M; Sigma), serotonin (5-HT, 10^{-9} to 10^{-6} M; Sigma), angiotensin II (Ang II, 10^{-11} to 10^{-6} M; Sigma), endothelin-1 (ET-1, 10^{-10} to 3.10^{-7} M; Sigma), noradrenaline (NA, 10^{-9} to 3.10^{-5} M; Sigma) or ATP (10^{-8} to 3.10^{-4} M; Sigma). In another set of experiments, TDA were preconstricted with 50 μM PE for 15 minutes and then incubated with cumulative concentrations of two different vasodilators: achetylcholine (Ach, 10^{-11} to 10^{-5} M; Sigma) or adenosine (Ado, 10^{-10} to 10^{-3} M; Sigma). Where indicated, the nitric oxide (NOS) inhibitor L-Nitro-Arginine Methyl Ester (L-NAME, 100μM; Sigma), the cyclooxygenase inhibitor indomethacin (3 μM; Sigma) or the intermediate conductance potassium channel blocker 1-[(2-chlorophenyl) diphenylmethyl]-1*H*-pyrazole (TRAM 34, 10 μM; Sigma) were added to the bath and applied intraluminally. For each vessel, the luminal diameter was measured after stabilization of the response to the given agonist.

Data analysis

Results are expressed in mean ± SEM. The degree of contraction was calculated according to the following equation: $D_{ago} \times 100/D_{max}$ where D_{ago} is the diameter of the TDA after application of a given concentration of a given agonist and D_{max} is the maximal diameter of the TDA measured at the end of each experiment by applying Krebs-HEPES calcium free supplemented with 2mM EGTA and 10 μM SNP to the TDA. The percentage of relaxation was calculated as followed: $(D_{Ach} - D_{PE}) \times 100/(D_{max} - D_{PE})$ where D_{Ach} is the diameter of the TDA after application of a given dose of Ach, D_{PE} is the diameter of the TDA 15 minutes after application of PE, D_{max} is the maximal diameter of the TDA determined as described above. Cumulative concentration response curves to the different agonists were fitted to the logistic equation using the Origin software in order to determine the maximum effect and the EC_{50} of each agonist as previously described (7). Data were compared using a one-way ANOVA and $P<0.05$ was considered significant.

Results

Histological properties of the TDA

Hematoxylin and eosin staining of the TDA revealed a thin tunica media separated from the intima by the internal elastic lamina (Figure 2A). The adventitia appeared thick and fibrous. One can also appreciate the abundance of adipose tissue around the TDA as well as the presence of a vein lying parallel to the TDA as described above and shown in Figure 1. The TEM technique allowed us to study the structure of the TDA wall with more precision and revealed the presence of an endothelium separated from 1 to 2 layers of SMC by an internal elastic lamina (Figure 2B). The SMC appeared to have an intercellular gap as previously published by us, an observation made multiple times in several vascular beds in the mouse (6). The smooth muscle cells surrounded the TDA in a wrapping manner (Figure 2C) and abundantly expressed the cell surface proteoglycan neuron-glial antigen-2 (NG2, Figure 2D), a key marker for arterial smooth muscle cells that is not expressed in venous smooth muscle cells (32, 53, 54).

In order to determine the innervation of the TDA, we stained for tyrosine hydroxylase and neuronal nitric oxide synthase which are present in adrenergic nerves and nitrergic nerves respectively (figure 3A and B respectively). Immunofluorescence experiments for these two

enzymes performed on whole mounted TDA revealed that the TDA is richly innervated with adrenergic nerves but poorly innervated with nitrergic nerves (Figure 3). To ensure that the lack of nNOS staining in the TDA was not due to our immunofluorescence protocol, we labeled a mouse mesenteric artery for nNOS, which revealed the presence of nitrergic nerves in this artery (Figure 3C).

Contractile properties of the TDA

The diameter of the TDA was measured at different intraluminal pressures in presence of calcium (active diameter) and in absence of calcium (passive diameter). Both active and passive diameters remained equal when the TDA was pressurized up to 50 mmHg (Figure 4A). However, for intraluminal pressures of approximately 60 mmHg to 140 mmHg, the TDA developed a myogenic tone with a maximum of 26.5 % at 130–140 mmHg (Figure 4B).

The response to different contractile agonists and vasodilators was studied on TDA in order to characterize the pharmacological properties of the TDA. Stimulation of the TDA with PE resulted in a maximal constriction of 41 ± 3 % of the maximal diameter at the dose of 10 μM with an EC_{50} of 1.28 ± 0.4 μM (Figure 5A and table 1). In comparison, TDA exhibited an enhanced constriction in response to NA (E_{max} = 32.6 ± 1.4 % of maximal diameter) with a slightly lower EC_{50} (0.67 ± 0.3 μM, Figure 5B and table 1). Stimulation of the TDA with Ang II resulted in the lowest constriction with a maximum effect (67.0 ± 4.3 % of maximal diameter) at approximately 30 nM Ang II and an EC_{50} of 4 ± 0.98 nM (Figure 5C and table 1). The TDA exhibited a low EC_{50} in response to ET-1 (4.3 ± 0.98 nM) and a high constriction at 0.1 μM (E_{max} = 37.2 ± 1.4 % of maximal diameter, Figure 5D and table 1). The TDA constriction in response to 5-HT is characterized by an E_{max} of 35.2 ± 2.1 % of maximal diameter and an EC_{50} of 66.7 ± 23 nM (Figure 5E and table 1). Regarding the stimulation to ATP, the TDA response revealed an EC_{50} of 32.3 ± 10.3 μM and a maximum effect of ATP at a concentration of 0.3 mM (E_{max} = 33.4 ± 4.9% of maximal diameter, Figure 5F, table 1).

The dilation to acetylcholine on TDA preconstricted with PE was maximal at 1 μM (97.8 ± 2.1 % relaxation) and the EC_{50} was 39.9 ± 13.0 nM (Figure 5G, table 1). In contrast, the TDA did not competely dilate in response to the highest dose of adenosine (approximately 80% of relaxation at 1 mM) and the plateau of the dose response curve was not reached, therefore, it was impossible for us to determine the EC_{50} and the E_{max} (Figure 5H).

Characterization of acetylcholine and phenylephrine responses

Cumulative concentrations of Ach were added to preconstricted TDA in presence of different inhibitors of endothelium-dependant pathways known to induce vasodilation. The maximum relaxation was decreased by the presence of L-NAME alone (blocking endothelium dependant relaxation through NO) or added to indomethacin (blocking the cyclooxygenase pathway) reducing the maximum relaxation from 98.2 ± 1.7 % in control condition to 71.0 ± 5.3 % and 72.9 ± 12.1 % in presence of L-NAME alone and with indomethacin respectively (Figure 6A and table 2). Conversely, the EC_{50} was increased from 46.5 ± 16.8 nM to 302.1 ± 81.1 nM and 136.7 ± 50.2 nM in presence of L-NAME alone and with indomethacin respectively (Figure 6A and table 2). The incubation of the TDA with TRAM 34 (blocking intermediate conductance potassium channels, IK_{Ca}) with L-NAME and indomethacin induced an additional reduction of Ach relaxation with an E_{max} of 37.0 ± 7.8% showing a role for IK_{Ca} in the L-NAME/indomethacin insensitive component of Ach response in the TDA (Figure 6A and table 2).

In control conditions, PE produced a constriction of approximately 50% of the maximal diameter, which was further reduced when the TDA was incubated with L-NAME alone (27.1 ± 2.4 % of the maximal diameter) and with indomethacin (29.0 ± 2.4 % of the maximal diameter, Figure 6B). The addition of TRAM 34 to L-NAME and indomethacin did not have any additional effect on PE response, reducing the diameter to 32.2 ± 3.3 % of the maximal diameter (Figure 6B).

The presence of aL-NAME/indomethacin insensitive component in Ach response and the role of NO in the PE response implied heterocellular communication between the smooth muscle and the endothelium that may be facilitated by myoendothelial junctions (MEJ) (12, 18, 38, 62, 67). Therefore, we used TEM and identified multiple contact points between smooth muscle cells and endothelial cells in the TDA (Figure 6C and D). The quantification of MEJs revealed that the TDA contains 1.63 MEJs per 10 μm of internal elastic lamina.

Discussion

Because the TDA may play a role in important physiological functions such as blood pressure and skeletal muscle blood flow regulation (31, 44), we sought to characterize the TDA, the artery where the spinotrapezius main feed artery originates in order to use it as a vascular model system (44). The mouse TDA is a long artery (about 10 to 15 mm) with a maximal internal diameter of approximately 250 μm with one layer of endothelial cells and one to two layers of smooth muscle cells. These characteristics are very similar to what has been reported on the first or second order of the mouse superior mesenteric artery (5, 20, 72). In addition, the staining of the TDA for tyrosine hydroxylase, the rate-limiting enzyme involved in the synthesis of catecholamines, revealed that the TDA is highly innervated with sympathetic nerves. This result is consistent with a previous report in the rat using a different technique for examining adrenergic fibers in which their density in the TDA was higher compared to the downstream feed arteries (including the main feed artery and the arcade arterioles of the spinotrapezius muscle), which makes the TDA the most innervated artery upstream the spinotrapezius muscle in the rat (61). The high degree of adrenergic innervation of the TDA is consistent with innervation of mesenteric arteries (26) and implicates that sympathetic activity on this artery could be especially important for physiological functions. However, our results indicated that the TDA is poorly innervated with nitrergic nerve compared to the mesenteric artery. Nitrergic innervation of the mesenteric artery has been shown to repress the adrenergic-dependent constriction in the rat (27) and to modulate the calcitonin gene related peptide response in mouse (47). The absence of nitrergic nerves in the TDA suggest that the neuronal control of vascular tone is different in the TDA compared to the mesenteric artery.

In an attempt to compare the TDA to other commonly used small arteries, we first studied the contraction developed by the TDA in response to increasing intraluminal pressures. The myogenic tone observed in the TDA appeared at the intraluminal pressure of 70–80 mmHg and the highest myogenic tone (about 25 to 30%) was observed at high intraluminal pressures (130–140 mmHg). These results were somewhat different compared to myogenic tone observed in the mouse second or third order of mesenteric artery or in the cremaster, where the maximum myogenic response is approximately the same as the one observed in the TDA, but the myogenic response is developed at lower intraluminal pressures (30, 40, 57, 74). This difference could be explained by the smaller size of the cremasteric and mesenteric arteries and suggests that the TDA may play a role in the regulation of blood flow at higher luminal pressures compared to the cremsteric and mesenteric arteries.

We further studied the contractile and dilatory abilities of the TDA in response to different vasoactive agents. The TDA response to PE and NA were comparable to those reported for

mouse in first to third order mesenteric artery (8, 13, 42, 48, 69). Additionally, we have shown in a previous report that the PE response in the TDA is exclusively mediated by the $\alpha 1_D$-adrenergic receptor which has been already demonstrated in different vascular beds such as the mesentery or the cremaster (6, 35, 70). Similarly, the response to 5-HT was consistent with observations in the mesentery where the EC_{50} varies between 68.5 nM to 1.42 μM according to different studies (22, 49, 50). The contraction induced by application of ET-1 and ATP to the TDA had a comparable E_{max} and EC_{50} to what has been reported in the second order of mouse mesenteric artery (40, 42, 43, 56, 71). However, the TDA exhibited a low response to Ang II compared to the other vasoconstrictors discussed above; indeed, the maximum effect for Ang II was approximately 70% of the maximal diameter whereas all the other vasoconstrictors induced a maximum effect between 30 and 40 % of the maximal diameter. However, this observation has also been reported in several papers in the second and third order of mesenteric artery (36, 43, 55, 68). Altogether, these results demonstrate that the TDA exhibit similar responses to contractile agents compared to those reported in the extensively studied mesenteric arteries, which makes the TDA an adequate vascular model system for vasoreactivity studies.

The vasodilatory properties of the TDA were assessed using two different agonists: Ach which induces an endothelium-dependent relaxation of the smooth muscle and Ado, known to provoke a direct relaxation of the smooth muscle through A_2 receptors (58). The relaxation of PE-preconstricted TDA in response to Ach dilated the TDA to its maximal diameter at 1 μM with an EC_{50} of 39.9 ± 13.0 nM (figure 5G and table 1) which is very similar to Ach dilation performed on mesenteric arteries or cremaster arteries (10, 23, 29, 39, 49). Conversely, the diameter of the TDA did not reach its maximal value after application of the highest dose of Ado that could be applied, due to the solubility limit of Ado. Also, the TDA appeared to be less sensitive to Ado than to Ach as the effect of Ach could be observed at low doses around 0.1 to 1 nM whereas the relaxant effect of Ado started at 0.1 to 1 μM (figure 5G and H). Similarly to Ach relaxation, the response to Ado was comparable to what has been observed in the mesenteric artery, showing that the TDA is a satisfactory vascular model system (60).

Our results showed that the NOS blocker L-NAME alone or in addition to the cyclooxygenase inhibitor, indomethacin, induced a decrease of the Ach relaxation which was further reduced by the blocker of intermediate conductance potassium channels (IK_{Ca}), TRAM 34, (Figure 6A). This result implies that the Ach response in the TDA is composed of an endothelium release of NO and involves the IK_{Ca} channels, which is consistent with observations reported in mesenteric artery and cremaster (10, 14, 19, 51, 73). The residual Ach dilation observed after blocking of NOS, cyclooxygenase and IK_{Ca} could be attributed to the small conductance potassium channels (SK_{Ca}) as their role in L-NAME/ indomethacine insensitive relaxation has been shown in the mouse mesentery and cremaster as well as in the hamster retractor muscle feed artery (10, 14, 17, 19, 51). The sensitivity of Ach response to L-NAME and to TRAM34 highly suggests that Ach relaxation in the TDA involves both NO release from endothelial cells as well as an endothelium-dependent hyperpolarization. As demonstrated in Figure 6B, the PE response is increased by inhibition of NO production whereas indomethacin and TRAM 34 did not exert any additional effect, suggesting that neither cyclooxygenase nor IK_{Ca} but only NO is involved in PE response in TDA (Figure 6B). The PE response has been studied by us and others and it has been suggested that the NO release is due to the passage of second messengers generated in the smooth muscle by PE to the endothelium through heterocellular communication at the myoendothelial junction (18, 67). Once the second messenger traverses the myoendothelial junction, it activates the eNOS pathway, releasing NO which feeds back on the smooth muscle resulting in the reduction of the contraction (18, 67).

The study of the Ach and PE components strongly suggest that heterocellular communication occurs between the smooth muscle and the endothelium in the TDA and our results demonstrated the presence of multiple contact points between the smooth muscle cells and the endothelial cells (i.e., myoendothelial junctions) in the TDA (18, 20, 29, 67). This observation, in addition to others reported by our laboratory, is consistent with Schmid-Schönbein's study in the rat TDA where the authors describe the presence of fenestrations in the elastic intima indicating endothelium and smooth muscle cells are in contact (64, 67).

In their study, the TDA appeared to be the first artery along the thoracodorsal arterial tree to present myoendothelial junctions (64). Indeed, the authors were unable to observe such fenestrations upstream of the TDA (in the axillary artery), whereas they became more frequent in the feed artery just proximal to the muscle (64). Their observations are consistent with previous reports showing very few to no MEJ in larger vessels and with the frequency of MEJs increasing with decreasing vessel size (28). The presence of MEJs in the mouse mesenteric and cremasteric arteries, as well as in the hamster retractor muscle feed artery, has been commonly observed by different investigators, including ourselves (20, 33, 57, 63).

The MEJ was first described by Rhodin as a cellular extension of an endothelial cell (primarily) or a smooth muscle cell pushing through the internal elastic lamina and being within close apposition (59). The controversy regarding the presence of a direct connection between the endothelium and smooth muscle, or a myoendothelial gap junction ("MEGJ"), was raised by scattered reports in the literature using TEM where incomplete contact between the two cell types was observed (25). This is not surprising considering the difficulty in using TEM to define a classical gap junction in a structure that is already smaller than 1 μm producing results which are suggestive at best and misleading at worst. For this reason, many people have used immuno-TEM, immunocytochemistry on "holes" in IEL, or dye coupling to define a connection between the two cell types (11, 20, 67). Although these techniques have their own drawbacks, they are more telling than classical TEM to define a "MEGJ." In this paper, we demonstrate the presence of multiple MEJs in the TDA but our TEM images do not provide any information on the presence of gap junctions at the MEJ. However, in regards to the TDA, we have previously demonstrated a key role for connexins at MEJs in the control of smooth muscle contraction by the endothelium in response to PE with data showing that this control is most due to the passage of inositol 1,4,5-trisphosphate through the MEJs (32, 33, 67).

Lastly, the TDA appears to possess satisfactory stability to make it a suitable vessel for *ex vivo* study (6, 67). The vessels maintain a consistent contractility for up to 8 hours, develop spontaneous tone, and react to a large range of vasoactive substances. Furthermore, the TDA is a long artery (10 to 15 mm) with very few collaterals which makes it convenient for cannulation experiments. The length of the TDA is also an advantage for experiments that requires a high quantity of material such as western blot, RT-PCR or co-immunoprecipitation (6, 67). Also, we have previously demonstrated that the TDA can be used for transfection using the electroporation method, after which it is still viable for 24 hours, showing that the TDA is a resistant tissue (6, 67).

In summary, the TDA is the primary vessel of the extensively studied spinotrapezius muscle arterial network, which we believe serves as an excellent model to study skeletal muscle physiology in health and disease states. In this report, we present evidence that the TDA is an ideal vascular model system as it behaves comparably to other small muscular arteries commonly studied such as the mesenteric arteries, with the advantage of being a long and robust vessel, which makes it adequate to study molecular and cellular mechanisms of vascular functions.

Acknowledgments

We are grateful to Brian R. Duling for careful review of the manuscript, the University of Virginia Histology Core for sectioning and staining of the TDA, Jan Redick and Stacey Guillot at the Advanced Microscopy Core services for TEM sectioning and technical help. This work was supported by National Institute of Health grant HL088554 (B.E.I.), American Heart Association Scientist Development Grant (B.E.I.), an American Heart Association postdoctoral fellowship (M.B.), a National Research Science Award postdoctoral fellowship grant 1F32HL103042-01 from the National Institutes of Health (A.C.S.) and a National Institutes of Health Cardiovascular Training Grant 5 T32 HL007284 (A.W.L.).

References

1. Bagher P, Davis MJ, Segal SS. Visualizing calcium responses to acetylcholine convection along endothelium of arteriolar networks in Cx40BAC-GCaMP2 transgenic mice. Am J Physiol Heart Circ Physiol. 2011; 301:H794–802. [PubMed: 21666122]
2. Bailey AM, O'Neill TJt, Morris CE, Peirce SM. Arteriolar remodeling following ischemic injury extends from capillary to large arteriole in the microcirculation. Microcirculation. 2008; 15:389–404. [PubMed: 18574742]
3. Bearden SE. Advancing age produces sex differences in vasomotor kinetics during and after skeletal muscle contraction. Am J Physiol Regul Integr Comp Physiol. 2007; 293:R1274–1279. [PubMed: 17626125]
4. Bearden SE, Payne GW, Chisty A, Segal SS. Arteriolar network architecture and vasomotor function with ageing in mouse gluteus maximus muscle. J Physiol. 2004; 561:535–545. [PubMed: 15388783]
5. Beleznai T, Takano H, Hamill C, Yarova P, Douglas G, Channon K, Dora K. Enhanced K+-channel-mediated endothelium-dependent local and conducted dilation of small mesenteric arteries from ApoE−/− mice. Cardiovasc Res. 2011; 92:199–208. [PubMed: 21690174]
6. Billaud M, Lohman AW, Straub AC, Looft-Wilson R, Johnstone SR, Araj CA, Best AK, Chekeni FB, Ravichandran KS, Penuela S, Laird DW, Isakson BE. Pannexin1 regulates alpha1-adrenergic receptor- mediated vasoconstriction. Circ Res. 2011; 109:80–85. [PubMed: 21546608]
7. Billaud M, Marthan R, Savineau JP, Guibert C. Vascular smooth muscle modulates endothelial control of vasoreactivity via reactive oxygen species production through myoendothelial communications. PLoS One. 2009; 4:e6432. [PubMed: 19649279]
8. Boedtkjer E, Praetorius J, Matchkov VV, Stankevicius E, Mogensen S, Fuchtbauer AC, Simonsen U, Fuchtbauer EM, Aalkjaer C. Disruption of Na+, HCO Formula Cotransporter NBCn1 (slc4a7) Inhibits NO-Mediated Vasorelaxation, Smooth Muscle Ca2+ Sensitivity, and Hypertension Development in Mice. Circulation. 2011; 124:1819–1829. [PubMed: 21947296]
9. Boegehold MA, Bohlen HG. Arteriolar diameter and tissue oxygen tension during muscle contraction in hypertensive rats. Hypertension. 1988; 12:184–191. [PubMed: 3410527]
10. Brahler S, Kaistha A, Schmidt VJ, Wolfle SE, Busch C, Kaistha BP, Kacik M, Hasenau AL, Grgic I, Si H, Bond CT, Adelman JP, Wulff H, de Wit C, Hoyer J, Kohler R. Genetic deficit of SK3 and IK1 channels disrupts the endothelium-derived hyperpolarizing factor vasodilator pathway and causes hypertension. Circulation. 2009; 119:2323–2332. [PubMed: 19380617]
11. Chadha PS, Liu L, Rikard-Bell M, Senadheera S, Howitt L, Bertrand RL, Grayson TH, Murphy TV, Sandow SL. Endothelium-dependent vasodilation in human mesenteric artery is primarily mediated by myoendothelial gap junctions intermediate conductance calcium-activated K+ channel and nitric oxide. J Pharmacol Exp Ther. 2011; 336:701–708. [PubMed: 21172909]
12. Chadha PS, Liu L, Rikard-Bell M, Senadheera S, Howitt L, Bertrand RL, Grayson TH, Murphy TV, Sandow SL. Endothelium-dependent vasodilation in human mesenteric artery is primarily mediated by myoendothelial gap junctions intermediate conductance calcium-activated K+ channel and nitric oxide. J Pharmacol Exp Ther. 336:701–708. [PubMed: 21172909]
13. Crassous PA, Flavahan S, Flavahan NA. Acute dilation to alpha(2)-adrenoceptor antagonists uncovers dual constriction and dilation mediated by arterial alpha(2)-adrenoceptors. Br J Pharmacol. 2009; 158:1344–1355. [PubMed: 19785657]
14. Damkjaer M, Nielsen G, Bodendiek S, Staehr M, Gramsbergen JB, de Wit C, Jensen BL, Simonsen U, Bie P, Wulff H, Kohler R. Pharmacological activation of KCa3.1/KCa2.3 channels

produces endothelial hyperpolarisation and lowers blood pressure in conscious dogs. Br J Pharmacol. 2011

15. de la Pena JA, Lineaweaver W, Buncke HJ. Microvascular transfers of latissimus dorsi and serratus anterior muscles in rats. Microsurgery. 1988; 9:18–20. [PubMed: 3393070]
16. de With MC, de Vries AM, Kroese AB, van der Heijden EP, Bleys RL, Segal SS, Kon M. Vascular anatomy of the hamster retractor muscle with regard to its microvascular transfer. Eur Surg Res. 2009; 42:97–105. [PubMed: 19088476]
17. Domeier TL, Segal SS. Electromechanical and pharmacomechanical signalling pathways for conducted vasodilatation along endothelium of hamster feed arteries. J Physiol. 2007; 579:175–186. [PubMed: 17138602]
18. Dora KA, Doyle MP, Duling BR. Elevation of intracellular calcium in smooth muscle causes endothelial cell generation of NO in arterioles. Proc Natl Acad Sci U S A. 1997; 94:6529–6534. [PubMed: 9177252]
19. Dora KA, Gallagher NT, McNeish A, Garland CJ. Modulation of endothelial cell KCa3.1 channels during endothelium-derived hyperpolarizing factor signaling in mesenteric resistance arteries. Circ Res. 2008; 102:1247–1255. [PubMed: 18403729]
20. Dora KA, Sandow SL, Gallagher NT, Takano H, Rummery NM, Hill CE, Garland CJ. Myoendothelial gap junctions may provide the pathway for EDHF in mouse mesenteric artery. J Vasc Res. 2003; 40:480–490. [PubMed: 14583659]
21. Engel BT, Sato A, Sato Y. Responses of sympathetic nerves innervating blood vessels in interscapular, brown adipose tissue and skin during cold stimulation in anesthetized C57BL/6J mice. The Japanese journal of physiology. 1992; 42:549–559. [PubMed: 1474676]
22. Fesus G, Dubrovska G, Gorzelniak K, Kluge R, Huang Y, Luft FC, Gollasch M. Adiponectin is a novel humoral vasodilator. Cardiovasc Res. 2007; 75:719–727. [PubMed: 17617391]
23. Gongora MC, Qin Z, Laude K, Kim HW, McCann L, Folz JR, Dikalov S, Fukai T, Harrison DG. Role of extracellular superoxide dismutase in hypertension. Hypertension. 2006; 48:473–481. [PubMed: 16864745]
24. Gray SD. Rat spinotrapezius muscle preparation for microscopic observation of the terminal vascular bed. Microvasc Res. 1973; 5:395–400. [PubMed: 4709736]
25. Gustafsson F, Mikkelsen HB, Arensbak B, Thuneberg L, Neve S, Jensen LJ, Holstein-Rathlou NH. Expression of connexin 37, 40 and 43 in rat mesenteric arterioles and resistance arteries. Histochemistry and cell biology. 2003; 119:139–148. [PubMed: 12610733]
26. Haddock RE, Hill CE. Sympathetic overdrive in obesity involves purinergic hyperactivity in the resistance vasculature. J Physiol. 2011; 589:3289–3307. [PubMed: 21576274]
27. Hatanaka Y, Hobara N, Honghua J, Akiyama S, Nawa H, Kobayashi Y, Takayama F, Gomita Y, Kawasaki H. Neuronal nitric-oxide synthase inhibition facilitates adrenergic neurotransmission in rat mesenteric resistance arteries. J Pharmacol Exp Ther. 2006; 316:490–497. [PubMed: 16236814]
28. Heberlein KR, Straub AC, Isakson BE. The myoendothelial junction: breaking through the matrix? Microcirculation. 2009; 16:307–322. [PubMed: 19330678]
29. Hill CE, Hickey H, Sandow SL. Role of gap junctions in acetylcholine-induced vasodilation of proximal and distal arteries of the rat mesentery. J Auton Nerv Syst. 2000; 81:122–127. [PubMed: 10869710]
30. Hoefer J, Azam MA, Kroetsch JT, Leong-Poi H, Momen MA, Voigtlaender-Bolz J, Scherer EQ, Meissner A, Bolz SS, Husain M. Sphingosine-1-phosphate-dependent activation of p38 MAPK maintains elevated peripheral resistance in heart failure through increased myogenic vasoconstriction. Circ Res. 2010; 107:923–933. [PubMed: 20671234]
31. Hudson S, Johnson CD, Marshall JM. Changes in muscle sympathetic nerve activity and vascular responses evoked in the spinotrapezius muscle of the rat by systemic hypoxia. J Physiol. 2011; 589:2401–2414. [PubMed: 21486771]
32. Isakson BE. Localized expression of an Ins(1,4,5)P3 receptor at the myoendothelial junction selectively regulates heterocellular Ca2+ communication. JCell Sci. 2008; 121:3664–3673. [PubMed: 18946029]

33. Isakson BE, Ramos SI, Duling BR. Ca2+ and inositol 1,4,5-trisphosphate-mediated signaling across the myoendothelial junction. CircRes. 2007; 100:246–254.
34. Jackson DN, Moore AW, Segal SS. Blunting of rapid onset vasodilatation and blood flow restriction in arterioles of exercising skeletal muscle with ageing in male mice. J Physiol. 2010; 588:2269–2282. [PubMed: 20375140]
35. Jackson WF, Boerman EM, Lange EJ, Lundback SS, Cohen KD. Smooth muscle alpha1D-adrenoceptors mediate phenylephrine-induced vasoconstriction and increases in endothelial cell Ca2+ in hamster cremaster arterioles. Br J Pharmacol. 2008; 155:514–524. [PubMed: 18604236]
36. Javeshghani D, Sairam MR, Schiffrin EL, Touyz RM. Increased blood pressure, vascular inflammation, and endothelial dysfunction in androgen-deficient follitropin receptor knockout male mice. J Am Soc Hypertens. 2007; 1:353–361. [PubMed: 20409866]
37. Johnstone SR, Ross J, Rizzo MJ, Straub AC, Lampe PD, Leitinger N, Isakson BE. Oxidized phospholipid species promote in vivo differential cx43 phosphorylation and vascular smooth muscle cell proliferation. Am J Pathol. 2009; 175:916–924. [PubMed: 19608875]
38. Kansui Y, Garland CJ, Dora KA. Enhanced spontaneous Ca2+ events in endothelial cells reflect signalling through myoendothelial gap junctions in pressurized mesenteric arteries. Cell Calcium. 2008; 44:135–146. [PubMed: 18191200]
39. Kassan M, Galan M, Partyka M, Trebak M, Matrougui K. Interleukin-10 Released by CD4+CD25+ Natural Regulatory T Cells Improves Microvascular Endothelial Function Through Inhibition of NADPH Oxidase Activity in Hypertensive Mice. Arterioscler Thromb Vasc Biol. 2011; 31:2534–2542. [PubMed: 21817097]
40. Kauffenstein G, Drouin A, Thorin-Trescases N, Bachelard H, Robaye B, D'Orleans-Juste P, Marceau F, Thorin E, Sevigny J. NTPDase1 (CD39) controls nucleotide-dependent vasoconstriction in mouse. Cardiovasc Res. 2009; 85:204–213. [PubMed: 19640930]
41. Khaki AA, Shoja MA, Khaki A. A rare case report of subscapular artery. Ital J Anat Embryol. 2011; 116:56–59. [PubMed: 21898975]
42. Ko EA, Amiri F, Pandey NR, Javeshghani D, Leibovitz E, Touyz RM, Schiffrin EL. Resistance artery remodeling in deoxycorticosterone acetate-salt hypertension is dependent on vascular inflammation: evidence from m-CSF-deficient mice. Am J Physiol Heart Circ Physiol. 2007; 292:H1789–1795. [PubMed: 17142347]
43. Kostenis E, Milligan G, Christopoulos A, Sanchez-Ferrer CF, Heringer-Walther S, Sexton PM, Gembardt F, Kellett E, Martini L, Vanderheyden P, Schultheiss HP, Walther T. G-protein-coupled receptor Mas is a physiological antagonist of the angiotensin II type 1 receptor. Circulation. 2005; 111:1806–1813. [PubMed: 15809376]
44. Lash JM. Arterial and arteriolar contributions to skeletal muscle functional hyperemia in spontaneously hypertensive rats. J Appl Physiol. 1995; 78:93–100. [PubMed: 7713849]
45. Lash JM. Contribution of arterial feed vessels to skeletal muscle functional hyperemia. J Appl Physiol. 1994; 76:1512–1519. [PubMed: 8045827]
46. Lash JM. Exercise training enhances adrenergic constriction and dilation in the rat spinotrapezius muscle. J Appl Physiol. 1998; 85:168–174. [PubMed: 9655771]
47. Legros E, Tirapelli CR, Carrier E, Brochu I, Fournier A, D'Orleans-Juste P. Characterization of the non-adrenergic/non-cholinergic response to perivascular nerve stimulation in the double-perfused mesenteric bed of the mouse. Br J Pharmacol. 2007; 152:1049–1059. [PubMed: 17906682]
48. Looft-Wilson RC, Ashley BS, Billig JE, Wolfert MR, Ambrecht LA, Bearden SE. Chronic diet-induced hyperhomocysteinemia impairs eNOS regulation in mouse mesenteric arteries. Am J Physiol Regul Integr Comp Physiol. 2008; 295:R59–66. [PubMed: 18448615]
49. Loufrani L, Henrion D. Vasodilator treatment with hydralazine increases blood flow in mdx mice resistance arteries without vascular wall remodelling or endothelium function improvement. J Hypertens. 2005; 23:1855–1860. [PubMed: 16148609]
50. Matsumoto T, Kobayashi T, Ishida K, Taguchi K, Kamata K. Enhancement of mesenteric artery contraction to 5-HT depends on Rho kinase and Src kinase pathways in the ob/ob mouse model of type 2 diabetes. Br J Pharmacol. 2010; 160:1092–1104. [PubMed: 20590603]

51. Milkau M, Kohler R, de Wit C. Crucial importance of the endothelial K+ channel SK3 and connexin40 in arteriolar dilations during skeletal muscle contraction. FASEB J. 2010; 24:3572–3579. [PubMed: 20427707]
52. Moore AW, Bearden SE, Segal SS. Regional activation of rapid onset vasodilatation in mouse skeletal muscle: regulation through alpha-adrenoreceptors. J Physiol. 2010; 588:3321–3331. [PubMed: 20624796]
53. Murfee WL, Rehorn MR, Peirce SM, Skalak TC. Perivascular cells along venules upregulate NG2 expression during microvascular remodeling. Microcirculation. 2006; 13:261–273. [PubMed: 16627368]
54. Murfee WL, Skalak TC, Peirce SM. Differential arterial/venous expression of NG2 proteoglycan in perivascular cells along microvessels: identifying a venule-specific phenotype. Microcirculation. 2005; 12:151–160. [PubMed: 15824037]
55. Osanai T, Tomita H, Kushibiki M, Yamada M, Tanaka M, Ashitate T, Echizen T, Katoh C, Magota K, Okumura K. Coupling factor 6 enhances Src-mediated responsiveness to angiotensin II in resistance arterioles and cells. Cardiovasc Res. 2009; 81:780–787. [PubMed: 19106112]
56. Perez-Rivera AA, Fink GD, Galligan JJ. Vascular reactivity of mesenteric arteries and veins to endothelin-1 in a murine model of high blood pressure. Vascul Pharmacol. 2005; 43:1–10. [PubMed: 15975530]
57. Potocnik SJ, McSherry I, Ding H, Murphy TV, Kotecha N, Dora KA, Yuill KH, Triggle CR, Hill MA. Endothelium-dependent vasodilation in myogenically active mouse skeletal muscle arterioles: role of EDH and K(+) channels. Microcirculation. 2009; 16:377–390. 371 p following 390. [PubMed: 19424929]
58. Ralevic V, Burnstock G. Receptors for purines and pyrimidines. Pharmacol Rev. 1998; 50:413–492. [PubMed: 9755289]
59. Rhodin JA. The ultrastructure of mammalian arterioles and precapillary sphincters. Journal of ultrastructure research. 1967; 18:181–223. [PubMed: 5337871]
60. Rubino A, Ralevic V, Burnstock G. Contribution of P1-(A2b subtype) and P2-purinoceptors to the control of vascular tone in the rat isolated mesenteric arterial bed. Br J Pharmacol. 1995; 115:648–652. [PubMed: 7582485]
61. Saltzman D, DeLano FA, Schmid-Schonbein GW. The microvasculature in skeletal muscle. VI. Adrenergic innervation of arterioles in normotensive and spontaneously hypertensive rats. Microvasc Res. 1992; 44:263–273. [PubMed: 1479927]
62. Sandow SL, Haddock RE, Hill CE, Chadha PS, Kerr PM, Welsh DG, Plane F. What's where and why at a vascular myoendothelial microdomain signalling complex. Clin Exp Pharmacol Physiol. 2009; 36:67–76. [PubMed: 19018806]
63. Sandow SL, Looft-Wilson R, Doran B, Grayson TH, Segal SS, Hill CE. Expression of homocellular and heterocellular gap junctions in hamster arterioles and feed arteries. Cardiovasc Res. 2003; 60:643–653. [PubMed: 14659810]
64. Schmid-Schonbein GW, Delano FA, Chu S, Zweifach BW. Wall structure of arteries and arterioles feeding the spinotrapezius muscle of normotensive and spontaneously hypertensive rats. Int J Microcirc Clin Exp. 1990; 9:47–66. [PubMed: 2323897]
65. Schmid-Schonbein GW, Firestone G, Zweifach BW. Network anatomy of arteries feeding the spinotrapezius muscle in normotensive and hypertensive rats. Blood Vessels. 1986; 23:34–49. [PubMed: 3708163]
66. Segal SS. Integration of blood flow control to skeletal muscle: key role of feed arteries. Acta Physiol Scand. 2000; 168:511–518. [PubMed: 10759588]
67. Straub AC, Billaud M, Johnstone SR, Best AK, Yemen S, Dwyer ST, Looft-Wilson R, Lysiak JJ, Gaston B, Palmer L, Isakson BE. Compartmentalized connexin 43 s-nitrosylation/denitrosylation regulates heterocellular communication in the vessel wall. Arterioscler Thromb Vasc Biol. 2011; 31:399–407. [PubMed: 21071693]
68. Su J, Palen DI, Boulares H, Matrougui K. Role of ACE/AT2R complex in the control of mesenteric resistance artery contraction induced by ACE/AT1R complex activation in response to Ang I. Mol Cell Biochem. 2008; 311:1–7. [PubMed: 18084722]

69. Syyong HT, Chung AW, van Breemen C. Marfan syndrome decreases Ca2+ wave frequency and vasoconstriction in murine mesenteric resistance arteries without changing underlying mechanisms. J Vasc Res. 2010; 48:150–162. [PubMed: 20926894]

70. Tanoue A, Koba M, Miyawaki S, Koshimizu TA, Hosoda C, Oshikawa S, Tsujimoto G. Role of the alpha1D-adrenergic receptor in the development of salt-induced hypertension. Hypertension. 2002; 40:101–106. [PubMed: 12105146]

71. Vial C, Evans RJ. P2X(1) receptor-deficient mice establish the native P2X receptor and a P2Y6-like receptor in arteries. Mol Pharmacol. 2002; 62:1438–1445. [PubMed: 12435812]

72. Virdis A, Colucci R, Neves MF, Rugani I, Aydinoglu F, Fornai M, Ippolito C, Antonioli L, Duranti E, Solini A, Bernardini N, Blandizzi C, Taddei S. Resistance artery mechanics and composition in angiotensin II-infused mice: effects of cyclooxygenase-1 inhibition. Eur Heart J. 2011

73. Wolfle SE, Schmidt VJ, Hoyer J, Kohler R, de Wit C. Prominent role of KCa3.1 in endothelium-derived hyperpolarizing factor-type dilations and conducted responses in the microcirculation in vivo. Cardiovasc Res. 2009; 82:476–483. [PubMed: 19218287]

74. Zhang J, Ren C, Chen L, Navedo MF, Antos LK, Kinsey SP, Iwamoto T, Philipson KD, Kotlikoff MI, Santana LF, Wier WG, Matteson DR, Blaustein MP. Knockout of Na+/Ca2+ exchanger in smooth muscle attenuates vasoconstriction and L-type Ca2+ channel current and lowers blood pressure. Am J Physiol Heart Circ Physiol. 2010; 298:H1472–1483. [PubMed: 20173044]

Perspectives

This study sought to characterize diverse functional and anatomical parameters of the mouse thoracodorsal artery, which supplies blood to the mouse spinotrapezius muscle. Our results show that the mouse thoracodorsal artery exhibit comparable functional and histological characteristics to other small muscular arteries such as the mouse mesenteric or cremasteric artery and the hamster retractor muscle feed artery. In sum, this artery represents a suitable vascular model for a mouse muscular artery which could be used in the future to study vascular function.

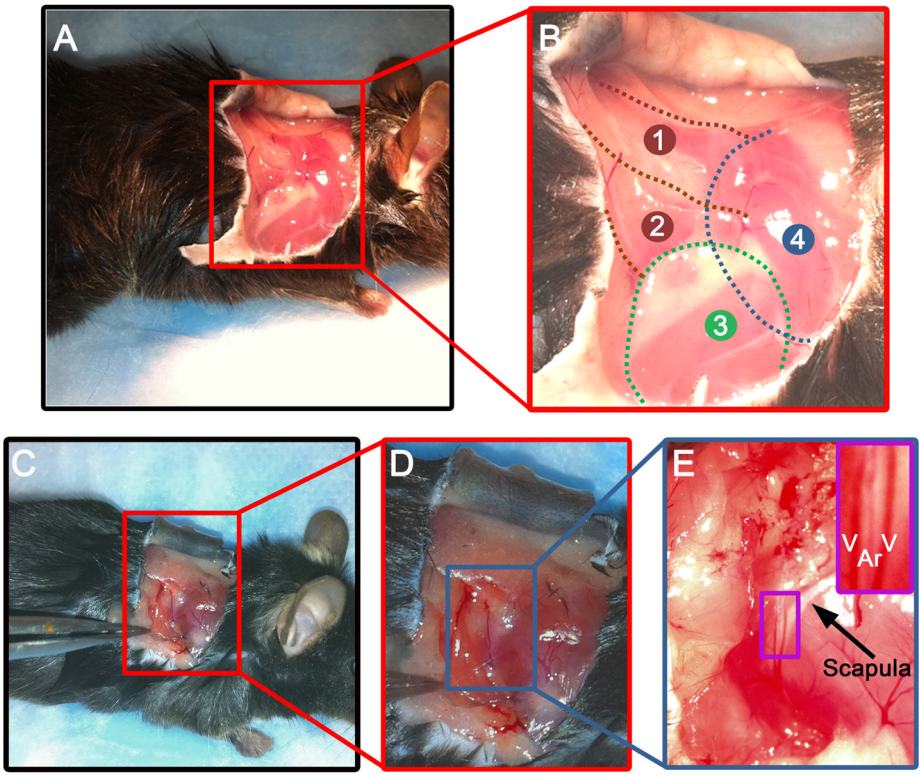

Figure 1. Isolation of the TDA

A, lateral view of the right shoulder of a mouse. **B**, enlargement of the red box shown in A describing the anatomy of the superficial muscles of the right shoulder of a mouse: 1: spinotrapezius muscle; 2: latissimus dorsi muscle; 3: triceps brachii muscle (forelimb); 4: position of the scapula. **C**, lateral view of the right shoulder of a mouse with a forceps pulling the latissimus dorsi muscle, revealing the TDA. **D**, enlargement of the red box shown in C. **E**, enlargement of the blue box in D. The purple box on the upper right shows a zoom in view of the TDA (Ar) surrounded by two veins (V) located on the caudal boarder of the scapula (designated by the arrow).

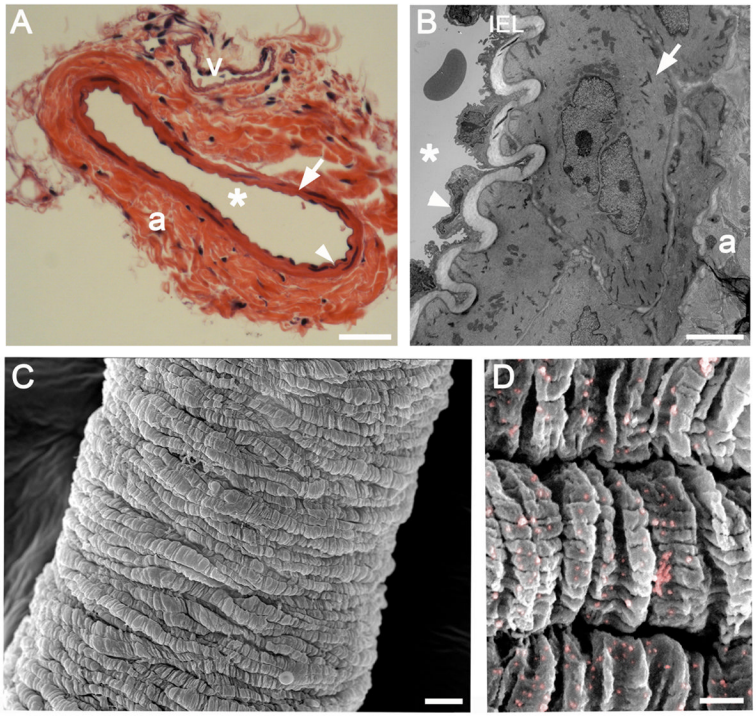

Figure 2. Histological properties of the TDA

A, hematoxylin and eosin staining of a TDA cross section. **B**, representative transmission electron microscopy image of a TDA transverse section. **C**, representative scanning electron microscopy (SEM) of a TDA. **D**, immuno-SEM of a TDA for NG-2 where nanogold beads were pseudocolored in pink for better visualization. Scale Bar in A: 50 μm. Scale bar in B: 5 μm. Scale bar in C: 10 μm. Scale bar in D: 1 μm. In A and B, the arrowheads indicates the endothelium, the arrows designate the smooth muscle, "*" indicates the lumen and "a": adventitia, "v: vein, IEL: Internal Elastic Lamina.

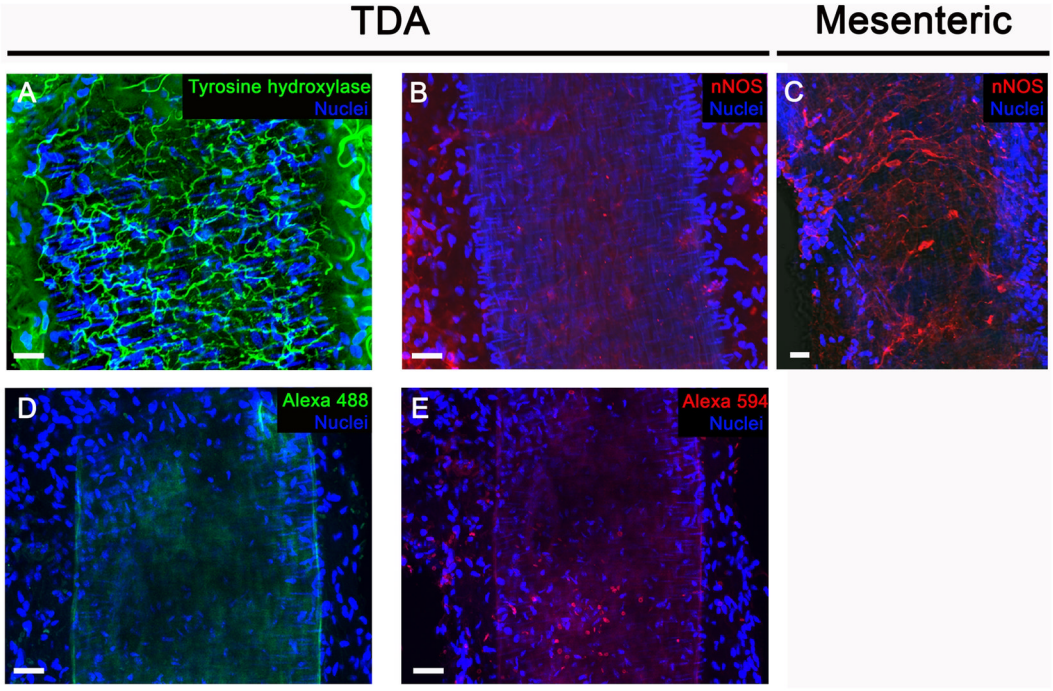

Figure 3. Innervation of the TDA

Immunofluorescent labeling of whole TDA with an antibody against tyrosine hydroxylase (**A**) or against nNOS (**B**). Mesenteric artery was used as a positive control for nNOS (C). Negative control using only the secondary antibody coupled to AlexaFluor 488 (**D**) or to AlexaFluor 594 (**E**). The nuclei are stained with DAPI (blue) in A through E. Scale bar: 20 μm.

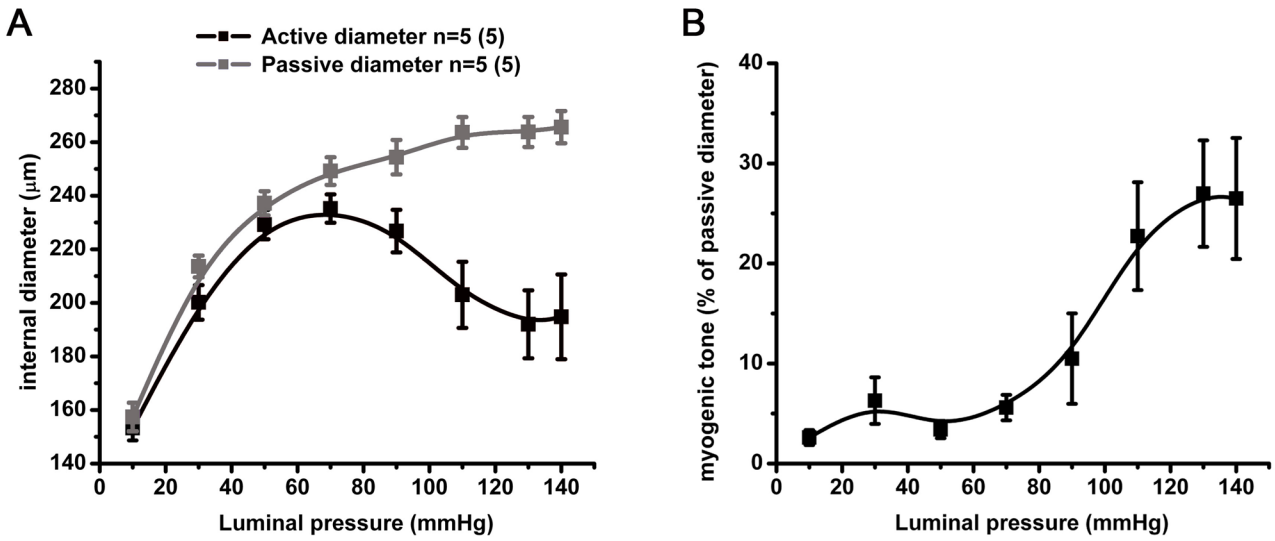

Figure 4. Mechanical properties of the TDA

A, active (black) and passive (grey) diameters developed in response to stepwise increase in luminal pressure applied to the TDA in presence or absence of calcium respectively. Active and passive diameters are expressed in μm and were used to calculate the myogenic tone (black) showed in **B**. n=5.

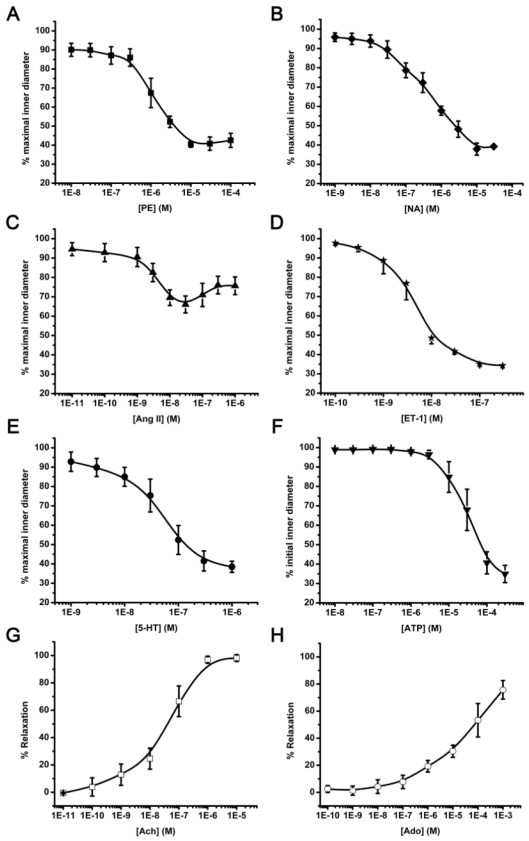

Figure 5. Contractile properties of the TDA in response to vasoactive agonists

Constriction induced by phenylephrine (**A**, n = 5), noradrenaline (**B**, n = 4), angiotensin-II (**C**, n = 7), endothelin-1 (**D**, n = 6), 5-HT (**E**, n = 4) ATP (**F**, n = 4). Relaxation induced by acetylcholine (**G**, n = 6) and adenosine (**H**, n = 5) on TDA preconstricted with phenylephrine (50 μmol/L). n values indicate the number of mice.

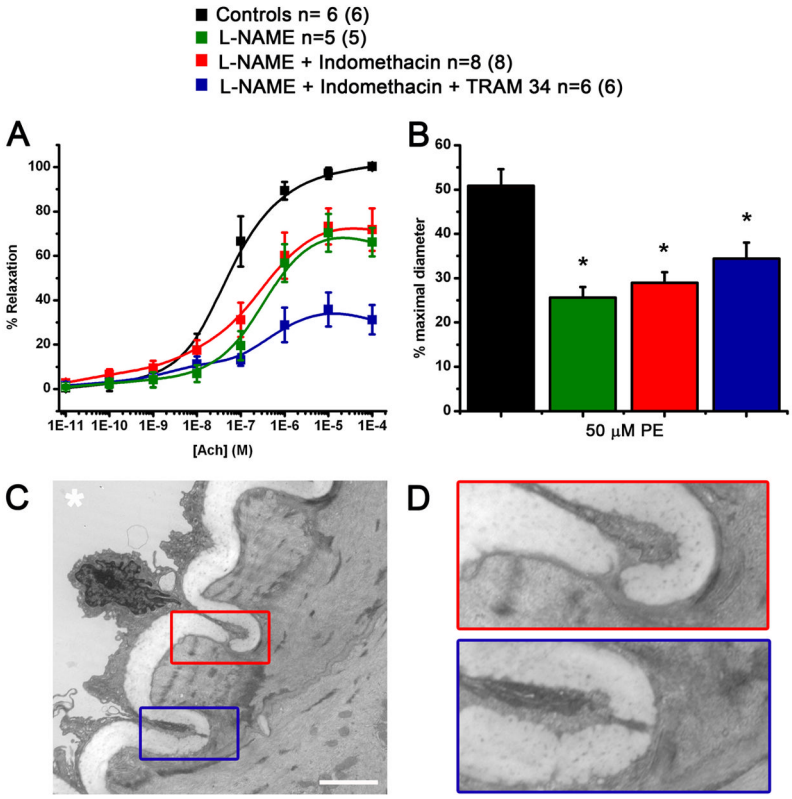

Figure 6. Characterization of the components of PE and Ach responses

Effect of L-NAME, indomethacin and TRAM 34 on response to cumulative concentrations of Ach (**A**) and on response to 50 μM PE (**B**). **C**, representative transmission electron microscopy image of a cross section of the TDA. **D**: enlargement of the red and blue boxes in C showing a myoendothelial junction. "*" indicates the lumen, scale bar in C is 2.5 μm. n values indicate the number of vessels and the number in parenthesis corresponds to the number of mice.

Table 1

Pharmacological properties of the TDA

Constriction to phenylephrine (PE), noradrenaline (NA), angiotensin II (Ang II), endothelin-1 (ET-1), serotonin (5-HT) and ATP as well as dilation to acetylcholine (Ach) were obtained in TDA. EC_{50} represents the concentration needed to produce 50% of the maximum effect (E_{max}). E_{max} is expressed as the percentage of maximal diameter. EC_{50} and E_{max} were calculated using the cumulative concentration response curves showed in Figure 5.

	PE	NA	Ang II	ET-1	5-HT	ATP	Ach
E_{max}	41.0 ± 3.0	32.6 ± 1.0	67.0 ± 4.3	37.2 ± 1.4	35.2 ± 2.1	33.4 ± 4.9	97.8 ± 2.1
EC_{50}	1.28 ± 0.4 μM	0.67 ± 0.3 μM	4.0 ± 1.6 nM	4.3 ± 0.98 nM	66.7 ± 23.0 nM	32.3 ± 10.3 μM	39.9 ± 13.0 nM

Table 2

Characterization of Ach dilation components

Cumulative concentrations of Ach were applied on TDA preconstricted with PE in presence of L-NAME (100 μM), indomethacin (3 μM) and TRAM 34 (10 μM). EC_{50} and E_{max} were calculated using the cumulative concentration response curves showed in Figure 6A.

	Control	L-NAME	L-NAME + Indomethacin	L-NAME + Indomethacin + TRAM 34
E_{max}	98.2 ± 1.7	71.0 ± 5.3 *	72.9 ± 12.1 *	37.0 ± 7.8 *#^
EC_{50}	46.5 ± 16.8 nM	302.1 + 81.1 nM *	136.7 + 50.2 nM	262.5 ± 76.2 nM

*, # and ^ indicate P< 0.05 compared to control, L-NAME and L-NAME + indomethacin respectively.